

Heart Rate Variability and the Acceleration Plethysmogram signals measured at rest

Mohamed Elgendi, Mirjam Jonkman and Friso DeBoer

School of Engineering and Information Technology,
Charles Darwin University, Australia

{Mohamed.Elgendi, Mirjam.Jonkman, Friso.DeBoer}@cdu.edu.au

Abstract. It is well-known that the electrocardiogram (ECG) is a non-invasive method that can be used to measure heart rate variability (HRV). Photoplethysmogram (PPG) signals also reflect the cardiac rhythm since the mechanical activity of the heart is coupled to its electrical activity. Photoplethysmography is a non-invasive, safe, and easy-to-use technique that has been developed for experimental use in vascular disease. A useful algorithm for *a*-wave detection in the acceleration plethysmogram (APG, the second derivative of the PPG) is introduced to determine the interval between successive heartbeats and heart rate variability. In this study, finger-tip PPG signals were recorded for twenty seconds from 27 healthy subjects measured at rest. The use of the *aa* interval in APG signals showed very promising results in calculating the HRV statistical indices, SDNN and rMSSD.

Keywords: Heart Rate, HRV, Photoplethysmogram, APG.

1 Introduction

The focus of this paper is the variation in the interval between consecutive heartbeats. Heart rate variability has become the conventionally accepted term to describe variations of both instantaneous heart rate and RR intervals in electrocardiogram (ECG) signals. A number of terms have been used in the literature to describe heart rate variability, for example, cycle length variability, heart period variability, RR variability, and RR interval tachogram. In this paper the acronym HRV will be used to describe the heart rate variability.

HRV measures the heart rate variations around the mean heart rate (HR). HRV provides information about the sympathetic-parasympathetic autonomic stability and consequently about the risk of unpredicted cardiac death. The traditional method to detect heart beats is detecting R peaks in ECG signals, a very promising tool to derive useful information about the hemodynamics as well as autonomic nerve system is the photoplethysmogram (PPG) signals. Accurate detection of inter-beat intervals from fingertip PPG signals is considered difficult. Ventricular pressure and other parameters of cardiac output however can influence the form and timing of the pulse

waveform. In addition, peripheral effects, such as changes in vascular tone, may also influence distal pulse peak detection.

These possible weaknesses of using the fingertip PPG signals in measuring HRV are mentioned by Bernston *et al.* [1]. Hence, they recommend the usage of RR intervals from ECG signals to determine inter-beat intervals. They do believe, however, that with a sophisticated peak detection algorithm the use of intra-arterial pressure pulses may be acceptable. According to them indirect measures, such as photoplethysmographic signals need further validation.

Giardino *et al.*[2] demonstrated that under resting conditions the distal pulse pressure, as shown in Fig.1 (a), is sufficient for determining the heart rate. However, they recommended extra studies that include test–retest reliability evaluation of different data collection techniques.

These reasons may explain the lack in investigating the use of PPG signals instead of ECG signals to measure the heart rate (HR) and the heart rate variability (HRV).

The PPG contour itself can be used to detect the heart beat and consequently HRV can be measured [3], as shown in Fig.1 (a) the two circles represent two consecutive heart beats with the smallest positive values in the PPG signal. However, reliable detection of heart beats from the PPG contour is challenging due to PPG noise and its interference incorporated nature [4].

To overcome the PPG contour analysis, the second derivative of photoplethysmogram, also called the acceleration plethysmogram (APG), has been introduced, as shown in Fig.1 (b); the two circles represent two consecutive heart beats with the largest positive values in the APG signal. Because the peaks in the APG signal are more clearly defined than the peaks in the PPG contour the heart rate can be more accurately detected using the APG.

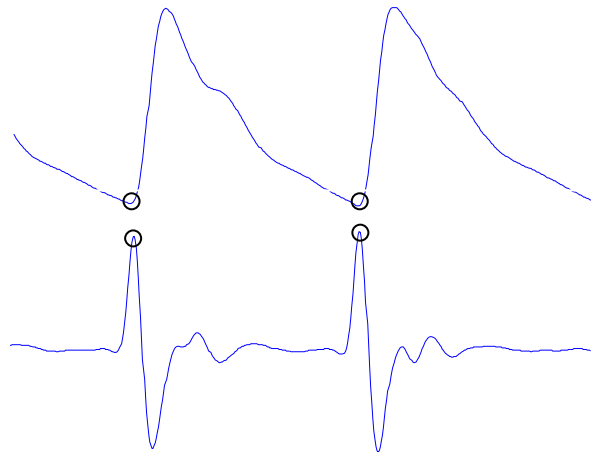


Fig. 1. Two successive beats in (a) fingertip photoplethysmogram (PPG) signal (b) second derivative wave of photoplethysmogram (APG) signal

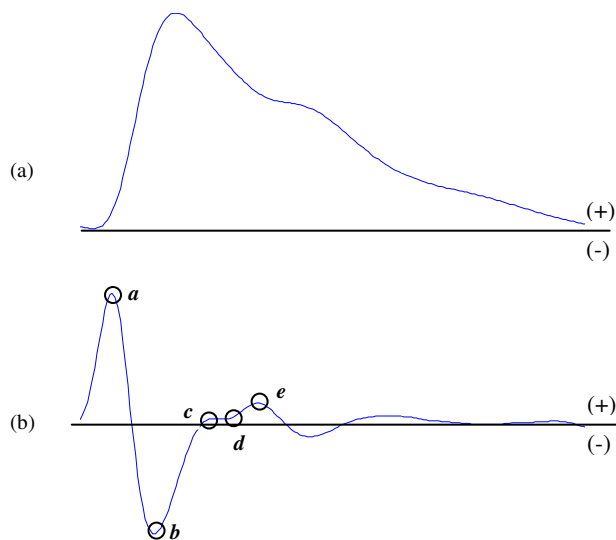


Fig. 2. One beat measurement (a) PPG (b) APG

A typical APG tracing of the cardiac cycle (heartbeat) consists of four systolic waves and one diastolic wave [5], namely *a*-wave (early systolic positive wave), *b*-wave (early systolic negative wave), *c*-wave (late systolic reincreasing wave), *d*-wave (late systolic redecreeasing wave) and *e*-wave (early diastolic positive wave), as shown in Fig.2 (b). The height of each wave was measured from the baseline, with the values above the baseline being positive and those under it negative. The first systolic wave, the *a*-wave seems the most suitable for heart rate calculations because of its amplitude and steepness.

Taniguchi *et al* [6] used the *aa* interval in the APG signals to determine HR instead of using the ECG when assessing the stress experienced by surgeons.

In the present study, our goal was to determine if variations in the APG signal can be used instead of the ECG for measuring the HRV. In addition, we investigate the relationship between HR and HRV at rest. In order to measure HRV using the APG signals, the accurate detection of *a* wave is an essential step. To date, there is still a lack of studies focusing on the automatic detection of *a*-waves in APG signals. Therefore, this investigation also aimed to develop a fast and robust algorithm to detect *a*-waves in APG signals. The APG waveform was measured in a population-based sample of healthy males at rest.

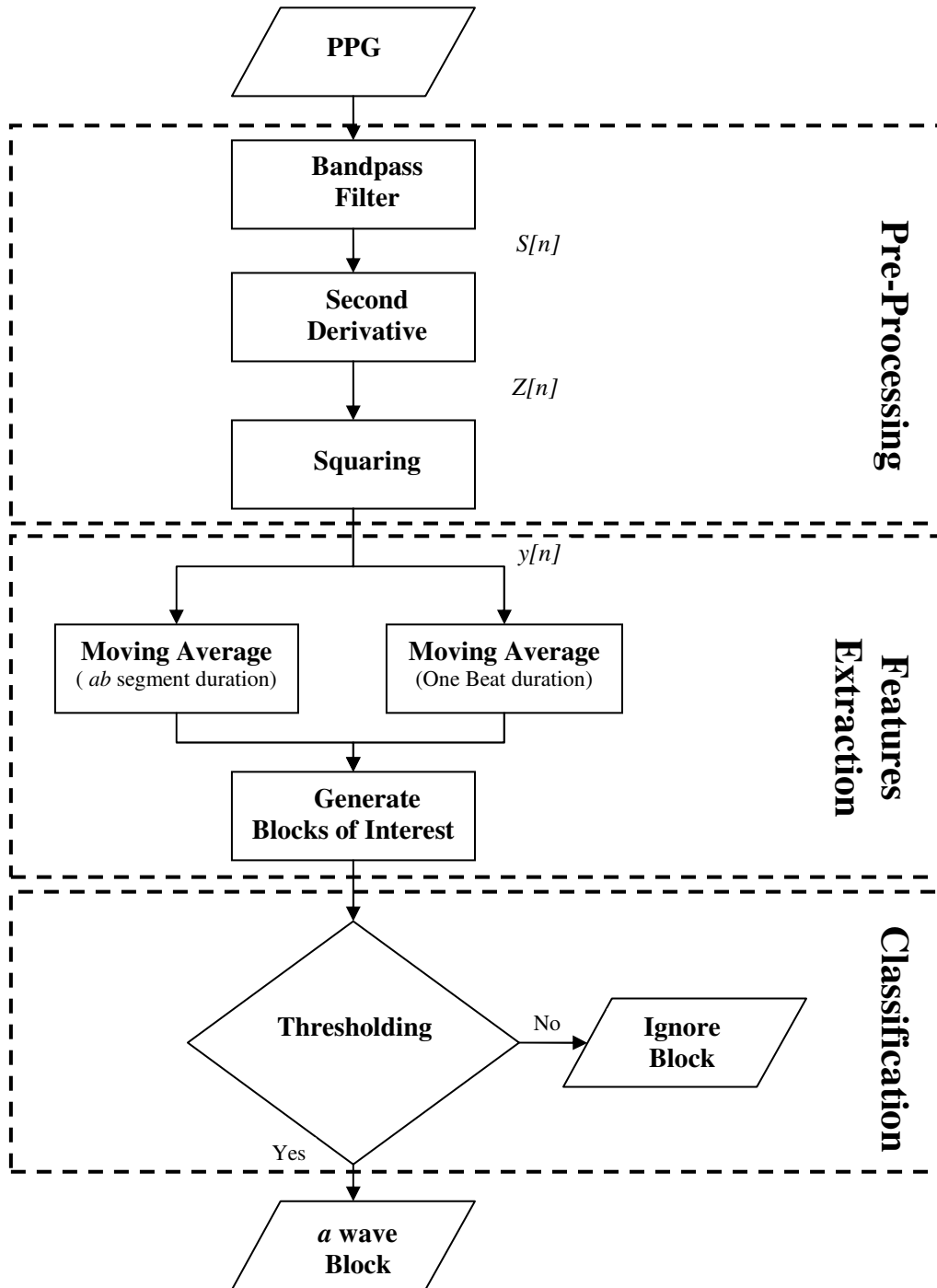


Fig. 3. Flowchart for new *a* wave detection algorithm

2 Data

The PPG data were collected as a minor part of a joint project between Charles Darwin University, Defence Science and Technology Organisation (DSTO) and the Department of Defence. The background of the entire project can be found in [7].

Twenty seven healthy volunteers (males) with a mean \pm SD age of 27 \pm 6.9. PPG were measured by a photoplethysmography (Salus PPG), with the sensor located at the cuticle of the second digit of the left hand. Measurements were performed while the subject was at rest on a chair. PPG data were collected at a sampling rate of 200 Hz. The duration of each data segment is 20 seconds [7].

The test was conducted from 20th of April to 5th of May 2006 at Northern Territory Institution of Sport (NTIS).

All procedures were approved by the ethics committee of Charles Darwin University. Informed consent was obtained from all volunteers.

3 Methodology

Accurate HRV calculation depends on accurate *a*-waves detection in the APG signals. The calculation of HRV from APG signals consists of two steps: detection of *a*-waves and calculation of the heart rate variability.

3.1 Detection of *a*-waves

The proposed *a* wave detection algorithm consists of three main stages: pre-processing, feature extractions and classification. The flowchart of the algorithm is shown in Fig. 3.

1) *Pre-processing*: In this stage the measured PPG signal is filtered, differentiated twice (to provide clean APG signals) and then squared (to provide a clear position for each heart beat).

A) Bandpass Filter: the baseline wander and high frequencies, which do not contribute to *a*-wave detection, have been removed by a second order Butterworth filter with passband 0.5-10 Hz. typically a recommended bandpass filter is a bidirectional Butterworth implementation [8]. This bandpass filter performs zero-phase digital filtering by processing the input data in both the forward and reverse directions. Moreover, Butterworth filters offer good transition band characteristics at low coefficient orders which make them efficient to implement [8].

A second order Butterworth filter with bandpass 0.5-10 Hz implemented by cascading a high pass and low-pass filter to remove the baseline wander and high frequencies which do not contribute to *a* and *b*-waves. Since one complete heart cycle takes approximately one second, the frequencies below 0.5 Hz can be considered as noise (baseline wander). The 10 Hz is chosen because most the energy of the PPG signal is below 10 Hz, as shown in Fig. 4(b).

The time domain representation of the filter is required because the filter is applied to PPG data samples, the filter can be defined [9] as

$$S[n] = \sum_{k=0}^N b_k PPG[n-k] - \sum_{k=1}^N a_k S[n-k] \quad (1)$$

where, a_k and b_k are the filter coefficients. $S[n]$ is the result of applying the bandpass filter to the input signal $PPG[n]$. Fig. 5(b) is the result of applying Butterworth filter to the original APG signal measured at rest shown Fig. 5(a).

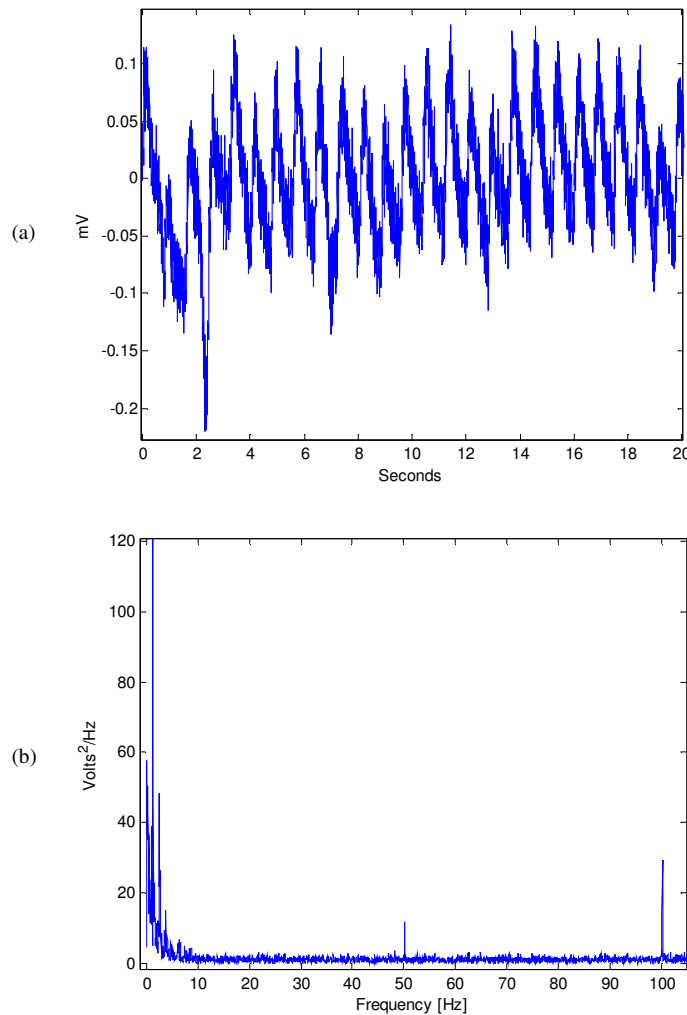


Fig. 4. Demonstrating the APG signals frequency bands (a) APG signal (b) the Fourier transform of the APG signal.

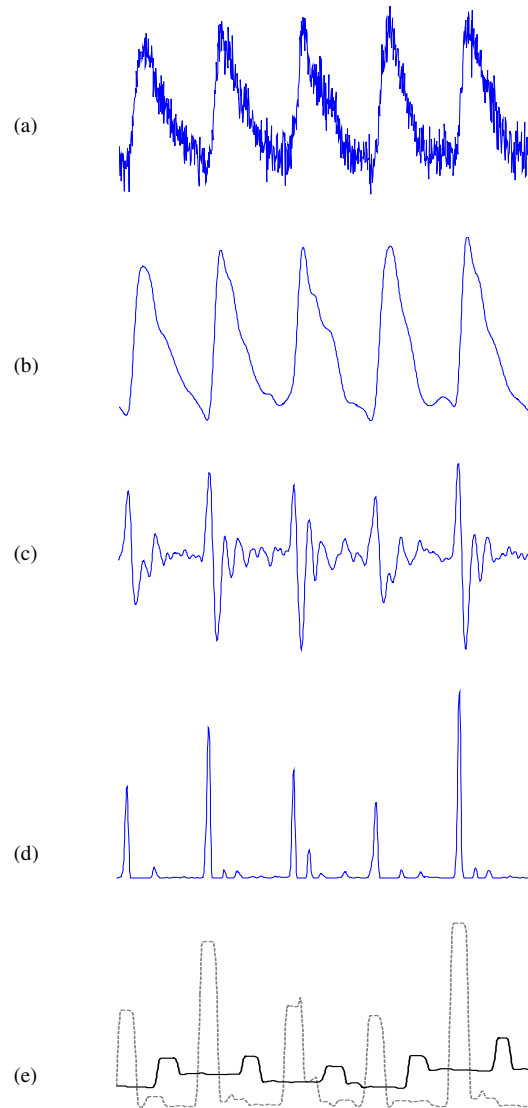


Fig. 5. Algorithm structure.(a) original PPG signal (b) filtered PPG signal with Butterworth bandpass filter (c) second Derivative of PPG which is APG signal (d) squaring the APG signal (e) generating blocks of interest using two moving averages to detect *a*-waves.

B) Second Derivative: To increase accuracy and the detection rate of the inflection points and make interpretation easier, the second derivative of photoplethysmogram, also called the acceleration plethysmogram (APG), has been introduced. Because the peaks in the APG signal are more clearly defined than the

peaks in the photoplethysmogram the heart rate can be more accurately detected using the APG, as shown in Fig. 5(c). In order to obtain the APG signal $Z[n]$, the second derivative will be applied to the filtered PPG signal $S[n]$.

$$\begin{aligned} S'[n] &= |S[n] - S[n-1]| \\ Z[n] &= |S'[n] - S'[n-1]| \end{aligned} \quad (2)$$

C) Squaring: At this stage the a -peak of the APG needs to be emphasized to distinguish it clearly for detection. This can be done by setting the negative parts of the signal equal to zero, followed by squaring the signal, resulting in $y[n]$.

$$\begin{aligned} \text{IF } Z[n] < 0 \text{ THEN} \\ &Z[n] = 0 \\ \text{END} \\ y[n] &= (Z[n])^2 \end{aligned} \quad (3)$$

2) *Features Extraction*: In this stage the squared APG will be processed by two moving averages to generate blocks of interest and then detect a -waves. The moving averages are low pass filters with filter coefficients equal to the reciprocal of the window size.

A) *First Moving Average*: The first moving average is used to emphasize the a and b wave, shown as the dotted line in Fig. 5(e) for APG signal measured at rest.

$$MA_{Peak}[n] = \frac{1}{W_1} (y[n - (W_1 - 1)/2] + \dots + y[n] + \dots + y[n + (W_1 - 1)/2]) \quad (4)$$

where $W_1 = 41$ which is the window width of ab segment.

B) *Second Moving Average*: The purpose of the second moving average, shown as the solid line in Fig. 5(e) for APG signal measured at rest, is used as a threshold for the output of the first moving average.

$$MA_{OneBeat}[n] = \frac{1}{W_2} (y[n - (W_2 - 1)/2] + \dots + y[n] + \dots + y[n + (W_2 - 1)/2]) \quad (5)$$

where $W_2 = 221$ is the window width of approximately one beat.

When the amplitude of the first moving average filter (MA_{Peak}) is greater than the amplitude of the second moving average filter ($MA_{OneBeat}$), that part of the signal is selected as a block of interest, as follows:

$$\begin{aligned} \text{IF } MA_{Peak}[n] > MA_{OneBeat}[n] \text{ THEN} \\ &Blocks[n] = 1 \\ \text{ELSE} \\ &Blocks[n] = 0 \\ \text{END} \end{aligned}$$

Table 1. *a*-waves detection performance and HRV indices calculated using the APG

| Record | No of beats | TP | FP | FN | SDNN | rMSSD |
|-----------|-------------|----|----|----|--------|-------|
| A1 | 26 | 26 | 0 | 0 | 0.024 | 0.013 |
| A2 | 24 | 24 | 0 | 0 | 0.033 | 0.030 |
| B1 | 17 | 17 | 0 | 0 | 0.080 | 0.108 |
| B2 | 26 | 26 | 0 | 0 | 0.086 | 0.043 |
| C2 | 20 | 20 | 0 | 0 | 0.105 | 0.118 |
| C3 | 20 | 20 | 0 | 0 | 0.105 | 0.142 |
| D2 | 22 | 22 | 0 | 0 | 0.059 | 0.051 |
| D3 | 19 | 19 | 0 | 0 | 0.063 | 0.074 |
| E1 | 22 | 22 | 0 | 0 | 0.045 | 0.056 |
| E2 | 22 | 22 | 0 | 0 | 0.045 | 0.056 |
| E3 | 19 | 19 | 0 | 0 | 0.095 | 0.144 |
| G2 | 30 | 30 | 0 | 0 | 0.019 | 0.013 |
| G3 | 19 | 19 | 0 | 0 | 0.056 | 0.033 |
| H3 | 23 | 23 | 0 | 0 | 0.058 | 0.051 |
| I1 | 22 | 22 | 0 | 0 | 0.034 | 0.037 |
| I2 | 17 | 17 | 0 | 0 | 0.052 | 0.079 |
| J2 | 23 | 23 | 0 | 0 | 0.0778 | 0.048 |
| L2 | 24 | 24 | 0 | 0 | 0.033 | 0.030 |
| L3 | 24 | 24 | 0 | 0 | 0.037 | 0.029 |
| N2 | 18 | 18 | 0 | 0 | 0.032 | 0.039 |
| N3 | 20 | 20 | 0 | 0 | 0.064 | 0.053 |
| O1 | 24 | 24 | 0 | 0 | 0.043 | 0.037 |
| O2 | 17 | 17 | 0 | 0 | 0.0459 | 0.050 |
| P1 | 26 | 26 | 0 | 0 | 0.083 | 0.073 |
| P2 | 20 | 20 | 0 | 0 | 0.129 | 0.137 |
| Q1 | 22 | 22 | 0 | 0 | 0.036 | 0.043 |
| Q2 | 18 | 18 | 0 | 0 | 0.140 | 0.161 |

Fig. 5(e) demonstrates the idea of using two filters to generate blocks of interest. Not all of the blocks are potential *a* and *b* waves. Some block are caused by noise and need to be eliminated.

The blocks associated with small width are considered as blocks caused by noise. Blocks which are smaller than half of the expected size for the *ab* interval are rejected. The expected size for the *ab* interval is based on the statistics for healthy adults, as described above. Blocks that is smaller than the expected width W_l that is expected for the *ab* interval will be rejected and the accepted blocks are considered to be containing *a*-wave.

The following statistical parameters were used to evaluate the algorithm:

$$\begin{aligned} Se &= \frac{TP}{TP+FN} \\ +P &= \frac{TP}{TP+FP} \end{aligned} \quad (6)$$

True Positive (TP): *a* wave has been classified as *a* wave.

False Negative (FN): *a* wave has been missed.

False Positive (FP): Non- *a* wave classified as *a* wave.

The sensitivity (*Se*) is the percentage of true *a* waves that were correctly detected by the algorithm. The positive predictivity (*+P*) is the percentage of detected *a* waves which are real *a* waves.

Table 1 shows the result of *a* waves detection in 27 different records of collected APG at rest, containing a total of 584 heart beats. The number of false negatives (FN) and false positives (FP) were zero. The overall average sensitivity for *a* waves detection was 100% and the positive predictivity was 100%.

3.2 HRV analysis

Once the location of each *a* wave is detected the duration of the consecutive *aa* intervals can be determined. Two time domain parameters are calculated and compared. These parameters are often used with ECG signals. The first parameter, the *SDNN*, is the standard deviation of the duration of heart beats; normal-to-normal R-to-R intervals in ECG signal. The second parameter, the *rMSSD*, is the root-mean square of the difference of successive heart beats or R-to-R intervals in ECG signals. Here, the RR interval is replaced by *aa* intervals. These were calculated in the previous step.

$$SDNN = \sqrt{\frac{1}{N} \sum_i (aa)^2 - \left(\frac{1}{N} \sum_i aa \right)^2} \quad (7)$$

$$rMSSD = \sqrt{\frac{1}{N} \sum_i (aa)^2} \quad (8)$$

where is *N* the total number of *aa* intervals, *i* is a counter.

4 Results

The *SDNN* and the *rMSSD* index were calculated for 27 subjects at rest, using recordings of the PPG of 20 seconds. The results are shown in table 1.

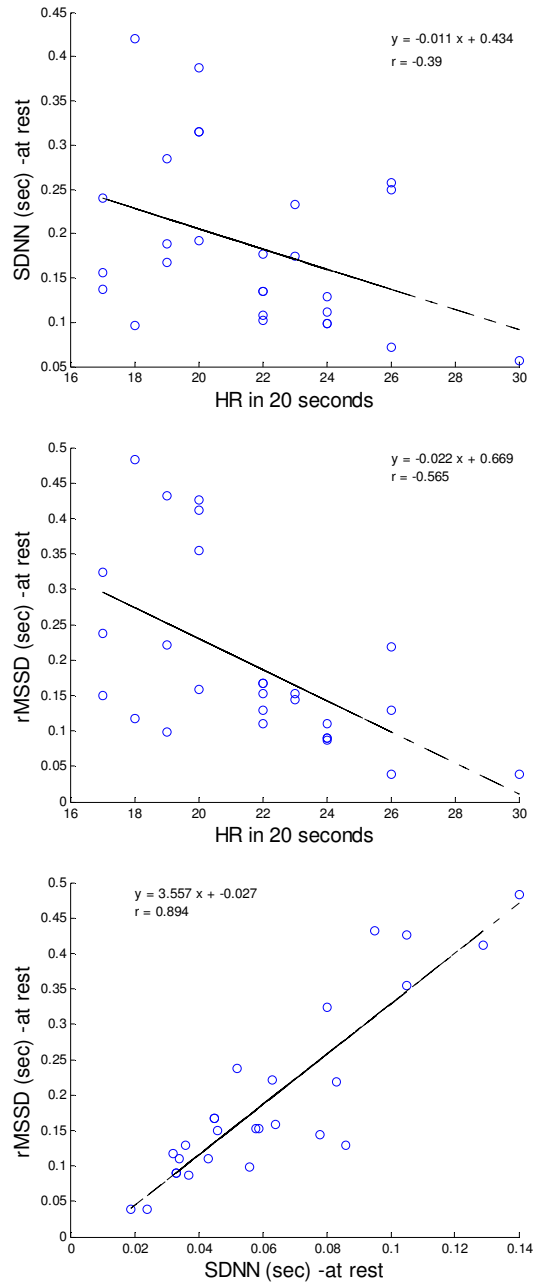


Fig. 6. Relations between (a) HR and *SDNN* (b) HR and *rMSSD* (c) *SDNN* and *rMSSD* calculated from APG signals for all subjects measured at rest.

In order to calculate the correlation between the heart rate and the HRV indices, the correlation coefficient is used as follows:

$$r = \frac{cov(x, y)}{\sigma_x \sigma_y} \quad (9)$$

where is r the correlation coefficient, $cov(x, y)$ is the covariance between data x and data y , σ_x is the standard deviation of data x and σ_y is the standard deviation of data y .

As can be seen from Fig. 6(a) and Fig. 6(b) there is a negative correlation between the heart rate and the heart rate variability indices. The $rMSSD$ index is more negative correlated with the HR ($r = -0.565$) than the $SDNN$ index ($r = -0.39$).

Fig. 6(c) shows the correlation between the two HRV indices. As can be expected, there is a strong positive correlation ($r = 0.894$).

Conclusion

The acceleration photoplethysmogram can be used to calculate heart rate variability. The accurate detection of a -waves leads to an accurate detection of aa interval and consequently reliable HRV measurement. Therefore, the proposed a -wave detection algorithm achieved an overall average sensitivity 100% and a positive predictivity was 100%. over 27 PPG records measured at rest, containing a total of 584 heart beats.

As discussed above, HRV indices which are normally used with ECG signals can also be applied to APG signals. The negative correlation between HR and both indices $SDNN$ and $rMSSD$ confirmed that the 20 seconds recordings of APG signal are suitable for short duration signal. As expected the $rMSSD$ index decreased more than $SDNN$. The reason is $rMSSD$ used to estimate the short-term components of HRV, related to the parasympathetic activity while $SDNN$ is related to overall HRV. There is a strong positive correlation between the two HRV indices, indicating that the 20 second APG recordings are sufficient to reliably measure the HRV. The usage of APG can be useful for HRV analysis and identification of individuals at risk.

Acknowledgment

The authors would like to thank Dr. Aya Matsuyama for collecting the data.

References

1. Berntson, G., et al.: Heart rate variability: origins, methods, and interpretive caveats. *Psychophysiology*. 34(6): p. 623-48 (1997)

2. Giardino, N., Lehrer, P., and Edelberg, R.: Comparison of finger plethysmograph to ECG in the measurement of heart rate variability. *Psychophysiology*, 39(2): p. 246-253 (2002)
3. Lu, S., et al.: Can photoplethysmography variability serve as an alternative approach to obtain heart rate variability information?. *J Clin Monit Comput.*, 22(1): p. 23-9 (2008)
4. Jianfeng, W., Zhiqian, Y., and Jianling, W.: An Improved Pre-processing Approach for Photoplethysmographic Signal. *IEEE-EMBS in Engineering in Medicine and Biology Society* (2005)
5. Takazawa, K., et al.: Clinical usefulness of the second derivative of a plethysmogram (acceleration plethysmogram). *Cardiology*, pp. 23:207-217 (1993)
6. Taniguchi, K., et al.: Evaluating the surgeon's stress when using surgical assistant robots. *Robot and Human interactive Communication. RO-MAN 2007. The 16th IEEE International Symposium on*, pp. 888-893 (2007)
7. Matsuyama, A.: ECG and APG Signal Analysis during Exercise in a Hot Environment, in *School of Engineering and Information Technology. Charles Darwin University: Darwin* (2009)
8. Oppenheim, A. and Shafer, R.: *Discrete-time Signal Processing*, NJ: Prentice Hall.
9. Rangayyan, R., M.: *Biomedical Signal Analysis A Case-Study Approach. IEEE Press Series on Biomedical Engineering*, ed. M. Akay., New York, U.S.A: John Wiley & Sons. 516 (2002)